Diagn Interv Radiol 2014; 20:185–192

NUCLEAR MEDICINE AND MOLECULAR IMAGING
ORIGINAL ARTICLE

Fluorine-18 fluorodeoxyglucose PET-CT for extranodal staging of non-Hodgkin and Hodgkin lymphoma

Özgür Ömür, Yusuf Baran, Aylin Oral, Yeşim Ceylan

PURPOSE
We aimed to evaluate the role of fluorine-18 fluorodeoxyglucose positron emission tomography-computed tomography (^{18}F-FDG PET-CT) involving care-dose unenhanced CT to detect extranodal involvement in patients with non-Hodgkin and Hodgkin lymphoma.

MATERIALS AND METHODS
Lymphoma patients (35 Hodgkin lymphoma, 75 non-Hodgkin lymphoma) who were referred for ^{18}F-FDG PET-CT imaging, following a diagnostic contrast-enhanced CT (CE-CT) performed within the last month, were included in our study. A total of 129 PET-CT images, and all radiologic, clinical, and pathological records of these patients were retrospectively reviewed.

RESULTS
In total, 137 hypermetabolic extranodal infiltration sites were detected by ^{18}F-FDG PET-CT in 62 of 110 patients. There were no positive findings by CE-CT that reflected organ involvement in 40 of 137 ^{18}F-FDG-positive sites. The κ statistics revealed fair agreement between PET-CT and CE-CT for the detection of extranodal involvement (κ=0.60). The organs showing a disagreement between the two modalities were the spleen, bone marrow, bone, and thyroid and prostate glands. In all lesions that were negative at CE-CT, there was a diffuse ^{18}F-FDG uptake pattern in the PET-CT images. The frequency of extranodal involvement was 51% and 58% in Hodgkin and non-Hodgkin lymphoma patients, respectively. There was a high positive correlation between the maximum standardized uptake values of the highest ^{18}F-FDG-accumulating lymph nodes and extranodal sites (r=0.67) in patients with nodal and extranodal involvement.

CONCLUSION
^{18}F-FDG PET-CT is a more effective technique than CE-CT for the evaluation of extranodal involvement in Hodgkin and non-Hodgkin lymphoma patients. PET-CT has a significant advantage for the diagnosis of diffusely infiltrating organs without mass lesions or contrast enhancement compared to CE-CT.

From the Department of Nuclear Medicine (Ö.Ö. ✉ *ozomur@yahoo.com*, A.O, Y.C.), Ege University School of Medicine, İzmir, Turkey; the Department of Molecular Biology and Genetics (Y.B.), İzmir Institute of Technology, İzmir, Turkey.

Received 28 April 2013; revision requested 10 July 2013; revision received 29 July 2013; accepted 31 July 2013.

Published online 10 January 2014.
DOI 10.5152/dir.2013.13174

Lymphomas are common hematological malignancies that predominantly affect the lymph nodes. However, both non-Hodgkin lymphoma (NHL) and Hodgkin lymphoma (HL) may affect any organ or tissue in the body. The lymphomatous infiltration of tissues other than the lymph nodes or lymphoid organs is described as extranodal lymphoma. The most common sites of lymphomatous infiltration are skin, stomach, spleen, Waldeyer's ring, central nervous system, bone, and lungs. The distribution and prevalence of affected organs vary according to the histological type and stage of the disease (1–4).

The presence of extranodal involvement is very important for staging NHL and HL. In general, extranodal involvement is more common in NHL than in HL, while it is frequently observed in recurrent disease and immune deficiency-related lymphomas (2–4). Moreover, primary and secondary extranodal diseases have different prognostic implications. Lymphomas that initially appear to have the bulk of the disease at extranodal sites are described in primary extranodal lymphoma and categorized as stage I or II. In secondary extranodal lymphoma, there is secondary involvement of the extranodal sites from primary nodal disease, which is categorized as stage III or IV. Except for the thymus and spleen, extranodal infiltration also indicates stage IV disease in HL. All of these data demonstrate the vital importance of diagnosis of extranodal lymphoma when designing treatment protocols at primary staging or restaging (3–5).

Cross-sectional anatomical imaging techniques, particularly computed tomography (CT), have been the primary modality for the diagnosis, staging, restaging, and follow-up of patients with lymphoma. However, these modalities have several limitations when detecting nodal or extranodal disease, because CT is based only on anatomical structural changes, such as the enlargement of lymph nodes or organs, presence of masses, and abnormal contrast enhancements. In NHL or HL, these structural abnormalities are detected in 60% to 90% of patients by CT (6–8). Normal-sized organs or nodes and diffuse lymphomatous infiltrations without mass effects reduce the sensitivity of anatomical imaging modalities.

Fluorine-18 fluorodeoxyglucose (^{18}F-FDG) positron emission tomography-computed tomography (PET-CT) is a hybrid imaging technique that simultaneously provides functional and anatomical information. This provides a significant advantage for the evaluation of lymphoproliferative malignancies, particularly for the detection of lymphomatous involvement in organs and nodes of normal size without any mass. Several studies suggest that the sensitivity and specificity of ^{18}F-FDG PET-CT for the assessment of nodal and extranodal involvement were higher than those

of standard contrast-enhanced CT (CE-CT) (3, 4, 7–11). These benefits make ^{18}F-FDG PET-CT the standard imaging technique for the initial staging, therapy response evaluation and restaging of patients with lymphoma.

The aim of this study was to evaluate the utility of ^{18}F-FDG PET-CT involving care-dose unenhanced CT for the detection of extranodal involvement in patients with NHL and HL. The ^{18}F-FDG PET-CT results were retrospectively compared with the diagnostic CE-CT data; follow-up results were used as a reference standard.

Materials and methods

Patients

From October 2011 to November 2012, 110 lymphoma patients (41 females, 69 males; mean age, 43.9±21.4 years) were included in this study. We evaluated those patients who had a diagnostic CE-CT evaluation within the previous month and were referred for ^{18}F-FDG PET-CT imaging. One hundred and twenty-nine PET-CT images, and all radiological, clinical, and pathological records of these 110 patients were retrospectively reviewed.

Thirty-five patients (13 females, 22 males; mean age, 43.5±21.5 years) had histologically proven HL, while 75 (28 females, 47 males; mean age, 43.9±21.4 years) had NHL. The histological classifications of the patients are presented in Table 1. Out of 129 ^{18}F-FDG PET-CT images, 52 were obtained for staging, 61 for therapy response evaluation, and 16 for restaging. PET-CT and CE-CT were performed after at least two cycles of chemotherapy, two weeks after the completion of chemotherapy or three months after the completion of radiotherapy to evaluate the therapeutic response.

The clinical and laboratory records of the patients were reviewed retrospectively in accordance and with the local ethics guidelines, and written informed consent was obtained from the subjects.

Imaging

Patients were injected intravenously with 250–450 MBq of ^{18}F-FDG at least six hours after the fasting period for ^{18}F-FDG PET-CT imaging. Approximately one hour after injection (40–60 min), PET-CT scanning was performed from the head to the proximal thigh using a clinical PET-CT system (Biograph high-definition 16-slice CT, Siemens Healthcare, Erlangen, Germany). CT scans were acquired using 80 kV tube voltage, 120 mA tube current, 0.6 s rotation time, 0.6 mm slice collimation, and kernel B31f for reconstruction. PET imaging was performed at 1 mm/min in bed position, and a 512×512 matrix and iterative reconstruction methods were used for the reconstruction of the PET images (attenuation-weighted, three iterations and 24 subsets, matrix size of 512, zoom of 10 isotropic, and CT resolution of 0.24 mm with 2 mm uniform resolution throughout the field of view).

PET and CT images were loaded on three-dimensional workstations for data analysis and visual evaluation. Attenuation-corrected and non-attenuation corrected images, as well as maximum intensity projections of PET, CT, and fusion PET-CT images, were evaluated visually on three orthogonal planes (coronal, sagittal, and axial). For quantitative evaluations, image analysis software (Syngo® Oncology Engine with TrueD™, Siemens Healthcare) was used. The ^{18}F-FDG uptake of the involved lymph nodes or tissues was quantified and identified as the maximum standardized uptake value (SUV_{max}) using the image analysis software program and the following formula: SUV=tissue radioactivity concentration (Bq/mL)/(injected dose [Bq]/body weight [g]).

CE-CT was performed independently in different centers equipped with multislice helical CT scanners within the last month (mean, 11±9 days) before PET-CT imaging.

All pathologic findings observed with ^{18}F-FDG PET-CT were directly compared with CE-CT. Detection of changes in density or pathologic contrast enhancement by CT in extralymphatic tissues and increased uptake of ^{18}F-FDG at these mass lesions (n=97) were accepted as extranodal infiltrations. In suspected lesions without typical CT findings indicating lymphomatous infiltration but with an increased uptake of ^{18}F-FDG (n=40), the presence of extranodal involvement was proved depending on the biopsy (n=25), magnetic resonance imaging (MRI) (n=3), or PET-CT data following the treatment observation (n=12). While a bone marrow biopsy was obtained during the staging of all cases, the biopsy results determined bone marrow infiltration for cases with diffused intramedullary bone uptake at ^{18}F-FDG PET-CT. The criteria for bone marrow infiltration in ^{18}F-FDG PET-CT were focal areas of increased tracer uptake or a diffusely increased uptake in patients not treated with drugs affecting the bone marrow. In cases with undetected lesions on the CE-CT and increased diffuse ^{18}F-FDG uptake in

Table 1. Histological classification and subtypes of the patients with Hodgkin and non-Hodgkin lymphoma

Histopathology	Subtypes	Number of patients	Female/Male
HL	Nodular sclerosing	22	9/13
	Mixed cellularity	11	4/7
	Lymphocyte-rich	2	0/2
High-grade NHL	Diffuse large B cell	48	18/30
	Peripheral T cell	3	0/3
	Burkitt lymphoma	2	2/0
	Anaplastic large cell	2	1/1
	Lymphoblastic	2	1/1
Low-grade NHL	Follicular	7	1/6
	Marginal zone	4	2/2
	Mantle cell	3	1/2
	MALT	2	2/0
	Chronic lymphocytic leukemia	2	0/2

HL, Hodgkin lymphoma; MALT, mucosa associated lymphoid tissue, NHL, non-Hodgkin lymphoma.

the spleen on the PET-CT before treatment, patients were accepted as splenic infiltration cases if they were not treated with chemotherapy or colony stimulating factor drugs, SUV levels of the spleen was over the liver, or spleen activity decreased together with the other uptake regions on post-therapy PET-CT. The diagnosis was confirmed with tissue biopsies in cases with increased ^{18}F-FDG uptakes indicating lymphomatous infiltrations in the thyroid gland, prostate, and stomach.

Statistical analysis

The agreement of PET-CT and CE-CT findings for extranodal lymphomatous involvement was assessed with the κ statistic. The agreements classified by the κ values were as follows: 0–0.20, very poor; 0.21–0.40, poor; 0.41–0.60, fair; 0.61–0.80, good; and 0.81–1.00, excellent. The Wilcoxon signed-rank test was used to compare the detectability of the lesions between the PET-CT and CE-CT. The correlations between the SUV_{max} of the lymph nodes and extranodal sites of the same patient and between patient groups were evaluated with Pearson's correlation analysis. The student's t test was used to evaluate the differences between the prevalence of extranodal involvement in different histological types and in the study group. Data were analyzed using the Statistical Package for the Social Sciences (SPSS) software (version 15.0 for Windows; SPSS Inc., Chicago, Illinois, USA). A P value of <0.05 was accepted as statistically significant.

Results

Sixty-two of 110 patients (56%) with lymphoma who had undergone ^{18}F-FDG PET-CT imaging and CE-CT evaluation had one or more extranodal sites. All 137 of the hypermetabolic extranodal infiltration sites were detected by ^{18}F-FDG PET-CT in these 62 patients. Positive findings reflected organ involvement, such as mass lesions or abnormal contrast enhancement, in 97 of 137 hypermetabolic extranodal sites upon CE-CT. There was no organ involvement found in 40/137 of the high ^{18}F-FDG accumulating extranodal sites with CE-CT. The extranodal infiltration sites of the patients, and ^{18}F-FDG PET-CT and CE-CT findings based on the lesion are presented in Table 2. The κ statistics revealed fair agreement between PET-CT and CE-CT for the detection of extranodal involvement (κ=0.60). Disagreements were observed between the two modalities regarding the spleen, bone marrow, bone, and thyroid and prostate glands (Table 2). All of these lesions with negative CE-CTs had diffuse ^{18}F-FDG uptake patterns in the PET-CT images.

Table 2. Number of patients with extranodal involvement detected by ^{18}F-FDG PET-CT and CE-CT

	High ^{18}F-FDG activity		Positive CE-CT		Negative CE-CT	
Extranodal site	NHL	HL	NHL	HL	NHL	HL
Lung	2	6	2	6	0	0
Pleura	6	1	6	1	0	0
Spleen	19	7	5	6	14	1
Bone	10	2	7	2	3	0
Bone marrow	11	6	0	0	11	6
Thyroid gland	2	1	0	0	2	1
Peritoneal cavity	5	0	5	0	0	0
Adrenal glands	3	0	3	0	0	0
Kidneys	3	2	3	2	0	0
Testicle	1	0	1	0	0	0
Prostate	2	0	1	0	1	0
Brain	3	1	3	1	0	0
Liver	2	5	1	5	1	0
Pancreas	2	0	2	0	0	0
Naso- or oropharynx, tonsils	11	3	11	3	0	0
Stomach	2	0	2	0	0	0
Thymus	4	0	4	0	0	0
Soft tissue and skin	12	3	12	3	0	0

CE-CT, contrast-enhanced computed tomography; ^{18}F-FDG PET-CT, fluorine-18 fluorodeoxyglucose positron emission tomography-computed tomography; HL, Hodgkin lymphoma; NHL, non-Hodgkin lymphoma.

The uptake regions were bone, bone marrow, spleen, liver, thyroid gland (Fig. 1), and prostate gland (Fig. 2), as detected by hypermetabolic involvement with ^{18}F-FDG PET-CT and then confirmed by biopsy, MRI, or follow-up results, with no detection of the lesion by CE-CT. There were diffused infiltrations and diffuse ^{18}F-FDG uptakes in all regions, except for the bone and liver.

On the patient-based evaluation, 24 of 110 patients had CE-CT negativity and hypermetabolic foci or focus in the extranodal organs. Because there were other hypermetabolic extralymphatic regions involved in 18 of 24 patients, the ^{18}F-FDG PET-CT data did not result in any change of the staging. However, in six cases, ^{18}F-FDG PET-CT caused an upstaging of the disease and changes in management through the demonstration of extranodal organ involvement that was undetected by CE-CT (Table 3). The percentages of patients downstaged and upstaged by PET-CT were 1.8% and 5.4%, respectively. The staging and post-therapeutic PET-CT findings of 24 patients with discordant ^{18}F-FDG PET-CT and CT results are presented in Table 3.

PET-CT resulted in a downstaging in two patients. There was extralymphatic involvement in the esophagus of one patient, as demonstrated by CT, while the other had higher involvement. ^{18}F-FDG uptake was not observed other than in the lymph nodes upon PET-CT in these cases; benign differences were confirmed by biopsy. No cases were reported as false positives based on PET-CT with the criteria we used, as explained in methods section.

Table 3. ^{18}F-FDG PET-CT findings of the patients' with discordant PET and CT results during staging and after treatment

Histological type	Extranodal involvement sites detected by ^{18}F-FDG PET-CT	Method of diagnostic confirmation	Post-therapeutic ^{18}F-FDG PET-CT results
Patients with disease upstaged by ^{18}F-FDG PET-CT			
NHL	Bone, bone marrow*	Biopsy (bone marrow)	Complete metabolic response
NHL	Bone (clivus)*, spleen*	MRI	Complete metabolic response
NHL	Prostate*	Biopsy	-
NHL	Spleen*, bone marrow*	Biopsy (bone marrow)	Complete metabolic, partial anatomic response
NHL	Spleen*, bone marrow*	Splenectomy	Progressive disease
NHL	Thyroid*, spleen*, bone marrow*	Biopsy (thyroid, bone marrow)	Complete metabolic response
Patients with disease stage unchanged by ^{18}F-FDG PET-CT			
HL	Bone, bone marrow*, spleen		Complete metabolic, partial anatomic response
HL	Bone marrow*, kidney, liver, spleen, thyroid*	Biopsy (bone marrow)	Complete metabolic, partial anatomic response
HL	Bone marrow*, kidney, lung, spleen*	Biopsy (bone marrow)	-
HL	Bone marrow*, lung, pleura		Progressive disease
HL	Bone marrow*, lung, spleen	Biopsy (bone marrow)	-
HL	Bone marrow*, spleen	Biopsy (bone marrow)	-
NHL	Bone (scapula)*, peritoneum, spleen*	MRI	-
NHL	Adrenal gland, bone marrow*, lung, peritoneum, spleen*, Waldeyer's ring	Biopsy (Waldeyer's ring)	Progressive disease
NHL	Bone, bone marrow*, liver*, spleen	MRI	-
NHL	Bone, bone marrow*, lung, pleura, soft tissue, spleen*	Biopsy (bone marrow)	Complete metabolic, partial anatomic response
NHL	Bone, bone marrow*, lung, spleen*		Complete metabolic and anatomic response
NHL	Bone marrow*, liver, lung, spleen*	-	Complete metabolic, partial anatomic response
NHL	Bone marrow*, liver, spleen*		Complete metabolic and anatomic response
NHL	Bone marrow*, lung, spleen*	Biopsy (bone marrow)	Complete metabolic, partial anatomic response
NHL	Diaphragm, peritoneum, pleura, spleen*, thyroid*	Biopsy (thyroid)	Complete metabolic, partial anatomic response
NHL	Nasopharynx, pancreas, spleen*	-	Partial metabolic and anatomic response
NHL	Spleen*, stomach	Biopsy (bone marrow, stomach)	Complete metabolic and anatomic response

*^{18}F-FDG(+)/CT(-) extranodal foci.
^{18}F-FDG PET-CT, fluorine-18 fluorodeoxyglucose positron emission tomography-computed tomography; HL, Hodgkin lymphoma; MRI, magnetic resonance imaging; NHL, non-Hodgkin lymphoma.

The relationship between the histological type of lymphoma and the prevalence and locations of extranodal sites are presented in Tables 2 and 4. The frequency of extranodal involvement was 51% (18/35) and 58% (44/75) in patients with HL and NHL, respectively. The most affected sites were the lungs, bone, bone marrow, spleen, and liver in HL, whereas the most affected sites in NHL were the spleen, bone, bone marrow, Waldeyer's ring, and soft tissue. Lung and liver involvement was significantly higher in HL than in NHL patients. However, the rates of lymphomatous infiltration of the bone, adrenal glands, testicle, prostate, pancreas, soft tissue, Waldeyer's ring, stomach, and thymus were significantly higher in NHL than in HL patients (Table 2). There was no significant correlation between histological type, grade, ^{18}F-FDG affinity (SUV) of the tumor and the detection of extranodal sites with ^{18}F-FDG PET-CT or CE-CT in the study group ($P < 0.05$).

In this study group, 29 patients had involvement in the cervical, thoracic, and abdominopelvic lymph nodes (three sites), while 27 patients had one or two lymphatic regions involved. Six patients had no lymph nodes involved. The SUV_{max} values of lymph nodes and extranodal sites were examined in patients having lymph node and extranodal involvements.

The mean SUV_{max} value was 23.3±13.2 for lymph nodes, which had the highest SUV_{max} in staging and restaging PET-CT scans, whereas the value was 7.4±2.8 in the post-therapy scans. The mean SUV_{max} for the extranodal infiltration sites was 20.6±14.2 in the staging/restaging PET-CT studies and 6.3±3.2 in the post-therapy PET-CT scans. There is a high positive correlation between the SUV_{max} values of the highest ^{18}F-FDG accumulating lymph nodes and extranodal sites (r=0.67) in patients with nodal and extranodal involvement.

Discussion

^{18}F-FDG PET-CT has been routinely used for staging, restaging, and therapy monitoring in patients with HL and high-grade NHL. This is a combined technique that presents the functional and anatomical data at the same imaging session. Various groups have used care-dose CT without the injection of intravenous iodinated contrast agent for attenuation, correction, or anatomical correlation. Previous studies revealed that ^{18}F-FDG PET-CT has a higher sensitivity and specificity than CE-CT in the evaluation of HL and high-grade NHL (3, 4, 7–11). Moreover, several studies have suggested that PET imaging with care-dose unenhanced CT alone might be sufficient for staging, therapy monitoring, or follow-up in patients with HL and aggressive NHL, except in special cases (7, 12). In this study, we aimed to evaluate the utility of ^{18}F-FDG PET with care-dose unenhanced CT to investigate the presence of extranodal spreading in NHL and HL patients.

Schaefer et al. (7) demonstrated that ^{18}F-FDG PET-CT with unenhanced CT has a higher sensitivity and specificity (100% and 90%, respectively) than CE-CT (88% and 50%, respectively) for the detection of extralymphatic involvement in patients with HL and high-grade NHL. Their results revealed that PET-CT is a more effective technique for the management of patients and might be sufficient, especially to exclude persistent or recurrent nodal-extranodal disease. In the current study, 137 hypermetabolic extranodal involvement sites, as confirmed by biopsy, radiological findings, or follow-up results, were detected with ^{18}F-FDG PET-CT in 62 patients with HL and NHL. Ninety-seven of these ^{18}F-FDG-positive extranodal sites (70%) had positive findings for organ involvement on CE-CT. However, there was no extranodal involvement in 40 of 137 hypermetabolic foci (30%) with high-dose CE-CT. Nearly, all of these CT-negative involvement sites had diffuse and nonfocal ^{18}F-FDG uptake patterns on PET-CT images, and the type of lymphomatous involvement was diffusely infiltrative without mass lesions. Contrast-enhanced CT-negative organs demonstrating the involvement of diffusely accumulating ^{18}F-FDG were the spleen, bone marrow, thyroid gland, and prostate. These results suggested that the involved organ and infiltration pattern were the most prominent factors for the detection of extranodal involvement with CE-CT. The results of this study noted that ^{18}F-FDG PET-CT has a significant advantage for the diagnosis of diffusely infiltrating organ involvements and is superior to CE-CT.

Several studies in the literature reported that ^{18}F-FDG PET-CT was an effective and reliable method to evaluate lymphomas in the pre-treatment and post-treatment periods; it was shown to be superior to CT for the observation of normal-sized but involved

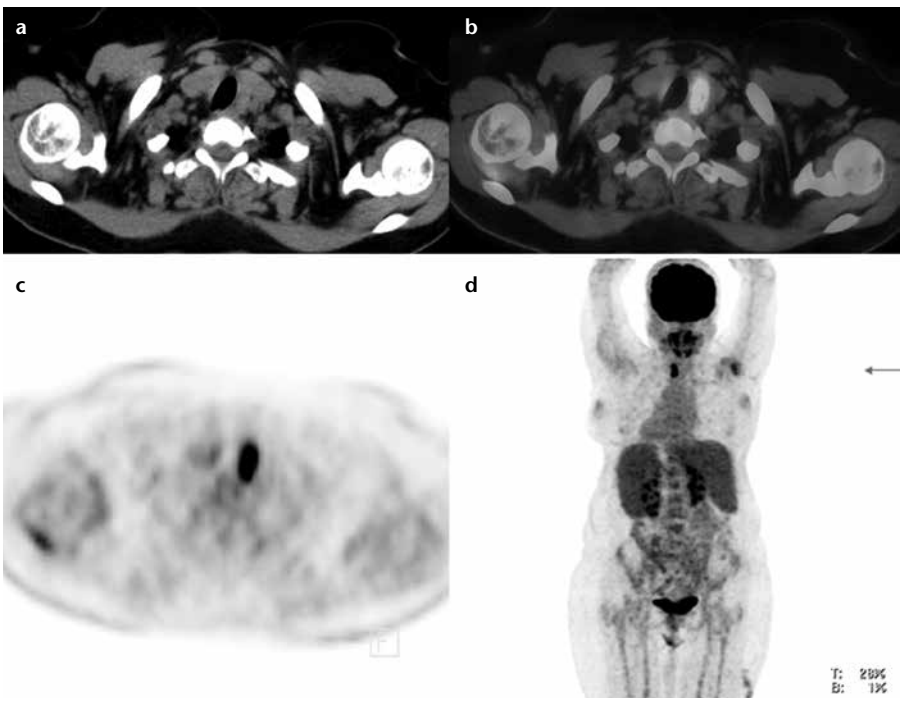

Figure 1. a–d. Unenhanced CT **(a)**, PET-CT **(b)**, PET **(c)**, and maximum intensity projection (MIP) **(d)** images for staging a 63-year-old patient with marginal zone non-Hodgkin lymphoma. There is diffuse ^{18}F-FDG uptake in the left lobe of the thyroid gland without CT findings. High ^{18}F-FDG accumulation is also observed in spleen, bone marrow, Waldeyer's ring, submandibular glands, and cervical lymph nodes on the MIP image **(d)**. Biopsy showed lymphomatous involvement in the bone marrow, thyroid gland, and Waldeyer's ring.

Table 4. Prevalence of extranodal involvement in different histological types and histological grades of lymphoma

Histological type	Extranodal involvement n/N (%)	Histological subtype/grade	Extranodal involvement n/N (%)
HL	18/35 (51)	Nodular sclerosing	10/22 (45.4)
		Mixed cellularity	8/11 (72.7)
		Lymphocyte-rich	0/2 (0)
NHL	44/75 (58)	High-grade	31/57 (54.3)
		Low-grade	13/18 (72)

HD, Hodgkin lymphoma; NHL, non-Hodgkin lymphoma.

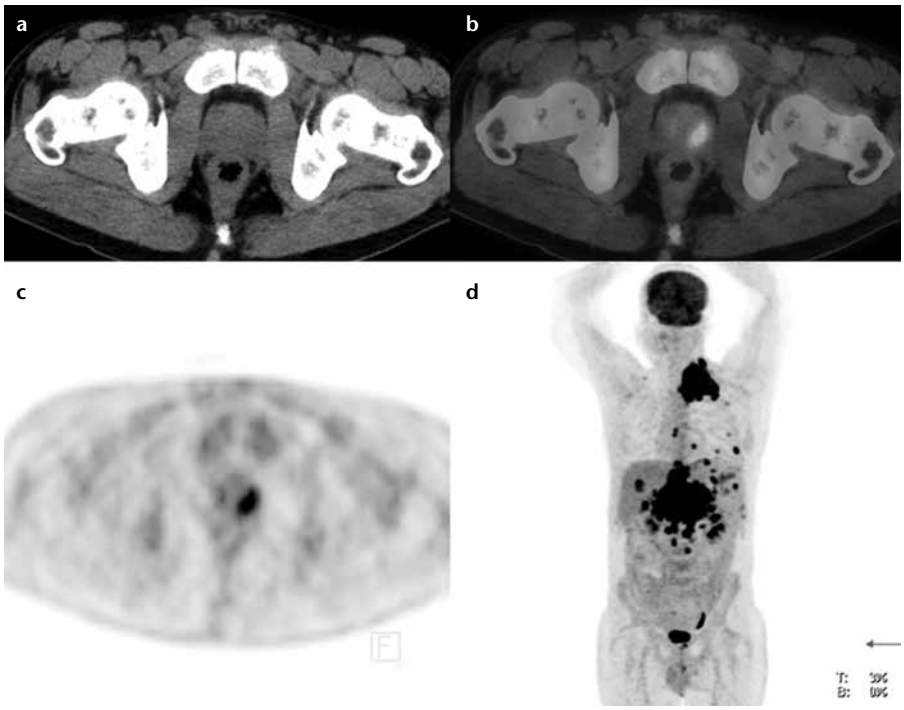

Figure 2. a–d. Unenhanced CT **(a)**, PET-CT **(b)**, PET **(c)**, and MIP **(d)** images for staging a 39-year-old patient with diffuse large B cell lymphoma. High ^{18}F-FDG uptake in the left part of the prostate gland is observed without CT findings. The patient also has conglomerated hypermetabolic lymph nodes in the cervical, thoracal, and abdominal regions, as well as liver, bone, and spleen involvement.

lymph nodes and diffusely infiltrated sites, such as the spleen or bone marrow (7, 9, 11–18). The role of PET-CT for splenic involvement in patients with lymphoma was evaluated by different studies. The results showed that the initial staging of splenic lymphomatous involvement, sensitivity and specificity of PET-CT were higher than those of the other diagnostic modalities alone (17, 18). PET-CT was also a highly sensitive and specific method for diagnosing bone marrow involvement in lymphomas (15, 16). However, its reliability differed depending on the histological type of the lymphoma, and a bone marrow biopsy is still needed (12, 16). In this study, the thyroid gland and prostate were the other organs with a diffuse infiltrative involvement and diffuse uptake of ^{18}F-FDG. Tissue biopsies were performed for a definitive diagnosis in these patients, and lymphomatous involvement was confirmed. Our results demonstrated that if there was any diffusely increased ^{18}F-FDG uptake in any organ, it must be evaluated for the presence of lymphomatous involvement by MRI, biopsy or follow-up studies.

The major limitations of ^{18}F-FDG PET-CT are its physiological uptake sites; among the common causes of false positive uptakes are infection, inflammation, and benign lesions. In such situations, the CT characteristics of the lesions must be examined. The urinary system, brain, stomach, and small and large bowel are physiological uptake or clearance sites for ^{18}F-FDG. In this study, all the patients diagnosed with lymphomatous involvement at such organs had positive findings on CE-CT or unenhanced CTs, while infiltration of the lymphoma was confirmed by histological evaluation. There were no false positive results from the ^{18}F-FDG PET-CT. These results suggest that high ^{18}F-FDG accumulations on the sites of the physiological ^{18}F-FDG distribution must be confirmed by anatomical imaging modalities, endoscopic studies and biopsies for a definitive diagnosis. Some studies have also reported that structural CT abnormalities and uptake intensities can improve the reliability of ^{18}F-FDG PET-CT for the differentiation of lymphomatous infiltration from physiological tracer activity, but the uptake pattern has not been found to be a reliable marker (3, 4, 8, 19–22). The Waldeyer's ring and lungs are also sites that have relatively high false positive results due to infectious or inflammatory reasons (23). Therefore, the CT characteristics, structural abnormalities, intensity and pattern of the ^{18}F-FDG uptake must be carefully evaluated. The recognition of abnormal findings at the Waldeyer's ring is important in making an accurate decision for the pathologic assessments. A detailed clinical history, such as whether PET-CT is a pretreatment or post-treatment, the time after the chemotherapy, and the treatments received, should be taken into consideration during the evaluation of PET-CT. PET-CT was obtained after the treatment, and all the other lymphatic-extralymphatic regions responded well to treatment. New ^{18}F-FDG uptake regions in the lung or oropharynx should be evaluated depending on the infection. In this study, no false positive results were detected in the lung or oropharyngeal regions upon PET-CT evaluations, based on the applied criteria.

The ^{18}F-FDG affinity of a tumor is one of the major decisive factors in the detection of pathologies by PET-CT. If structural abnormalities are not carefully examined, infiltrated lymph nodes or organs may be overlooked in low ^{18}F-FDG-avid tumors, such as low-grade NHLs. In this study, there was no significant correlation between the histological type or grade of lymphoma and the detection of extranodal involvement with ^{18}F-FDG PET-CT or CE-CT. In low ^{18}F-FDG-avid tumors, as in low-grade NHLs, lower detection rates were expected more than in high-grade NHLs. However, the detected lesion rates in our low-grade NHL cases were close to the high-grade NHL cases. This could have resulted from the inclusion of patients in advanced stages of the disease. These patients were referred to our clinic for PET-CT imaging to restage the disease, including relapse findings, by CT.

In the current study, the frequency of extranodal involvement was 51% and 58% in patients with HL and NHL, respectively. The most frequent extranodal infiltrations were detected in the lung, bone marrow, spleen, and liver in

patients with HL, while the most common infiltrations in NHL patients were in the spleen, bone marrow, Waldeyer's ring, and soft tissue. In the literature, extranodal involvement has been reported in 25% to 50% of NHL and in 5% to 20% of HL patients (1–7). In our group, the frequency of extranodal involvement was higher than that reported in other series. There were some differences in the distribution of the affected sites. While the frequency of liver and lung involvement has been shown to be quite low in the literature, our results revealed that there was a higher lymphomatous infiltration in HL cases than in NHL cases in these organs (3, 4, 8). Differences in geographical or genetic features, patient selection criteria for referring PET-CT imaging, stage or aggressiveness of the tumor, and a relatively higher number of patients with secondary or recurrent disease might be responsible for this outcome. We obtained similar results regarding the frequency of extranodal uptake and the affected organs in NHL cases (3, 4, 8).

The SUV has been widely used for the semiquantitative measurement of normalized tissue radioactivity concentrations in PET-CT studies. This parameter is one of the major advantages of PET-CT especially in the follow-up of patients with ^{18}F-FDG-avid tumors (24, 25). The mean or maximum SUV of all voxels within the region of interest (SUV_{mean} and SUV_{max}, respectively) has been used for the measurement of the cellular metabolism of a tumor with PET-CT. For the treatment response, the SUV_{max} value was usually preferred because it is independent from the defined region of interest (24, 25). An early treatment response, even before anatomical changes could be visualized, can also be evaluated with SUV_{max} (25, 26). Oh et al. (26) reported that the SUV_{max} is an independent prognostic factor in primary extranodal diffuse large B cell lymphomas. They examined cutoff values of the SUV_{max}, mean tumor diameters and the relation between these parameters and clinical outcomes in patients with diffuse large B cell lymphomas presenting in extranodal organs, lacking in or demonstrating only minor lymph node involvement. Therefore, no possible relationship between the SUV_{max} of lymph nodes and the involved organs could be evaluated (26). To our knowledge, no previous study has examined the possibility of a relationship between the SUV_{max} of the involved lymph node, and the extranodal organs in the same patient with lymphoma. In this study, we detected a high positive correlation between the SUV_{max} values of the highest ^{18}F-FDG-accumulating lymph nodes and extranodal sites. These data may indicate that the highest SUV_{max} of the nodal sites can help in the differential diagnosis of organ infiltrations over other ^{18}F-FDG-avid benign conditions, such as inflammation or infection, especially in patients with high ^{18}F-FDG accumulation in extranodal sites without mass lesions.

Our results demonstrate that ^{18}F-FDG PET-care-dose unenhanced CT is a more sensitive imaging modality than CE-CT alone for the evaluation of the extranodal involvement of patients with NHL and HL. This modality has substantial superiority to CE-CT in the diagnosis of diffusely infiltrated organs without mass lesion or contrast enhancement, such as the spleen, bone marrow, thyroid gland, and prostate gland. However, accurate criteria must be used for the evaluation of ^{18}F-FDG PET-CT, and structural abnormalities must be examined carefully to manage patients accurately.

In conclusion, in lymphoma patients with nodal involvement and suspicious ^{18}F-FDG PET-CT findings for extranodal infiltration, SUV_{max} of extralymphatic organs that is close to the SUV_{max} of maximum ^{18}F-FDG-accumulating lymph nodes can be considered as lenfomatous infiltration.

Conflict of interest disclosure

The authors declared no conflicts of interest.

References

1. Chua SC, Rozalli FI, O'Connor SR. Imaging features of primary extranodal lymphomas. Clin Radiol 2009; 64:574–588. [CrossRef]
2. Even-Sapir E, Lievshitz G, Perry C, Herishanu Y, Lerman H, Metser U. Fluorine-18 fluorodeoxyglucose PET/CT patterns of extranodal involvement in patients with non-Hodgkin lymphoma and Hodgkin's disease. Radiol Clin North Am 2007; 45:697–709. [CrossRef]
3. Pates FM, Kalkanis DG, Sideras PA, Serafini AN. FDG PET/CT of extranodal involvement in non-Hodgkin lymphoma and Hodgkin disease. Radiographics 2010; 30:269–291. [CrossRef]
4. Guermazzi A, Brice P, Kerviler E, et al. Extranodal Hodgkin disease: spectrum of disease. Radiographics 2001; 21:161–179. [CrossRef]
5. Zucca E, Conconi A, Cavalli F. Treatment of extranodal lymphomas. Best Pract Res Clin Haematol 2002; 15:533–547. [CrossRef]
6. Ping L. Staging and classification of lymphoma. Semin Nucl Med 2005; 35:160–164. [CrossRef]
7. Schaefer NG, Hany TF, Tverna C, et al. Non-Hodgkin lymphoma and Hodgkin disease: coregistered FDG PET and CT at staging and restaging do we need contrast-enhanced CT? Radiology 2004; 232:823–829. [CrossRef]
8. Leite NP, Kased N, Hanna RF, et al. Cross-sectional imaging of extranodal involvement in abdomino-pelvic lymphoproliferative malignancies. Radiographics 2007; 27:1613–1634. [CrossRef]
9. Seam P, Juweid ME, Chenson BD. The role of FDG-PET scans in patients with lymphoma. Blood 2007; 110:3507–3516. [CrossRef]
10. Juweid ME. Utility of positron emission tomography (PET) scanning in managing patients with Hodgkin lymphoma. Hematology 2006; 2006:259–265. [CrossRef]
11. Juweid ME. FDG-PET/CT in lymphoma. Methods Mol Biol 2011; 727:1–19. [CrossRef]
12. Schaefer NG, Tverna C, Strobel K, Wastl C, Kurrer M, Hany TF. Hodgkin disease: diagnostic value of FDG PET/CT after first-line therapy—is biopsy of FDG-avid lesions still needed? Radiology 2007; 244:257–262. [CrossRef]
13. Moog F, Bangerter M, Diederichs CG, et al. Extranodal malignant lymphoma: detection with FDG PET versus CT. Radiology 1998; 206:475–481.
14. Stumpe KD, Urbinelli M, Steinert HC, Glanzmann C, Buck A, von Schulthess GK. Whole-body positron emission tomography using fluorodeoxyglucose for staging of lymphoma: effectiveness and comparison with computed tomography. Eur J Nucl Med 1998; 25:721–728. [CrossRef]
15. Pakos EE, Fotopoulos AD, Ioannidis JPA. 18F-FDG PET for evaluation of bone marrow infiltration in staging of lymphoma: a meta-analysis. J Nucl Med 2005; 46:958–963.
16. Wu L, Chenb F, Jiangc X, Gua H, Yina Y, Xua J. 18F-FDG PET, combined FDG-PET/CT and MRI for evaluation of bone marrow infiltration in staging of lymphoma: a systematic review and meta-analysis. Eur J Radiol 2012; 81:303–311. [CrossRef]
17. Rini JN, Leonidas JC, Tomas MB, Palestro CJ. 18F-FDG PET versus CT for evaluating the spleen during initial staging of lymphoma. J Nucl Med 2003; 44:1072–1074.

18. de Jong PA, van Ufford HM, Baarslag HJ, et al. CT and 18F-FDG PET for noninvasive detection of splenic involvement in patients with malignant lymphoma. Am J Roentgenol 2009; 192:745–753. [CrossRef]
19. Radan L, Fischer D, Bar-Shalom R, et al. FDG avidity and PET/CT patterns in primary gastric lymphoma. Eur J Nucl Med Mol Imaging 2008; 35:1424–1430. [CrossRef]
20. Ilıca AT, Kocaçelebi K, Savaş R, Ayan A. Imaging of extranodal lymphoma with PET/CT. Clin Nucl Med 2011; 36:127–138. [CrossRef]
21. Lee WK, Lau EWF, Duddalwar VA, Stanley AJ, Ho YY. Abdominal manifestations of extranodal lymphoma: spectrum of imaging findings. Am J Roentgenol 2008; 191:198–206. [CrossRef]
22. Barrington SF, O'Doherty MJ. Limitations of PET for imaging lymphoma. Eur J Nucl Med Mol Imaging 2003; 30:117–127. [CrossRef]
23. Tan LHC. Lymphomas involving Waldeyer's ring: placement, paradigms, peculiarities, pitfalls, patterns and postulates. Ann Acad Med Singapore 2004; 33:15S–26S.
24. Adams MC, Turkington TG, Wilson JM, Wong TZ. A systematic review of the factors affecting accuracy of SUV measurements. Am J Roentgenol 2010; 195:310–320. [CrossRef]
25. Benz MR, Evilevitch V, Allen-Auerbach MS, et al. Treatment monitoring by 18F-FDG PET/CT in patients with sarcomas: interobserver variability of quantitative parameters in treatment-induced changes in histopathologically responding and nonresponding tumors. J Nucl Med 2008; 49:1038–1046. [CrossRef]
26. Oh MY, Oh SB, Seoung HG, et al. Clinical significance of standardized uptake value and maximum tumor diameter in patients with primary extranodal diffuse large B cell lymphoma. Korean J Hematol 2012; 47:207–212. [CrossRef]